Journal of Molecular Catalysis B: Enzymatic 61 (2009) 39–46

Contents lists available at ScienceDirect

Journal of Molecular Catalysis B: Enzymatic

journal homepage: www.elsevier.com/locate/molcatb

Characterization of recombinant thiamine diphosphate-dependent phosphonopyruvate decarboxylase from *Streptomyces viridochromogenes* Tü494

Sandra Johnen[1], Georg A. Sprenger*

Institut für Biotechnologie 1, Forschungszentrum Jülich GmbH, D-52425 Jülich, Germany

ARTICLE INFO

Article history:
Available online 5 April 2009

Keywords:
Thiamine diphosphate
Phosphonopyruvate
Decarboxylase
Site-directed mutagenesis
Thiamine binding site

ABSTRACT

Phosphonopyruvate decarboxylase (PPDC) catalyzes the thiamine diphosphate-dependent non-oxidative decarboxylation of phosphonopyruvate to phosphonoacetaldehyde and carbon dioxide. The enzyme of *S. viridochromogenes* Tü494 was expressed as a recombinant fusion protein with an N-terminal 10× histidine-tag in *Escherichia coli* cells, and was purified to homogeneity by nickel affinity chromatography. The biochemical properties of the recombinant enzyme were characterized, measuring phosphonoacetaldehyde formation by two newly developed coupled enzyme assays. PPDC has a high affinity to its cofactors ThDP, and Mg^{2+} (both $K_m \sim 40\,\mu M$). The metal ions Ca^{2+} and Mn^{2+} ($K_m \sim 3\,\mu M$) could substitute for Mg^{2+}. In coupled enzyme assays at pH 8.0 (HEPES buffer) and at 30 °C, PPDC followed Michaelis–Menten kinetics with phosphonopyruvate, with a K_m value of $3.2 \pm 0.35\,\mu M$ and a v_{max} value of 0.81 ± 0.01 U/mg. Neither pyruvate, β-hydroxypyruvate, nor fluoropyruvate served as alternative substrates. Gel filtration chromatography indicated a molecular mass of $72{,}100 \pm 220$ Da. Taking into account a subunit size of about 43,600 Da, the quaternary structure of the Ppd appears to be homodimeric.

A comparison with the pyruvate decarboxylase (PDC) from *Zymomonas mobilis* allowed the identification of several amino acid residues, whose potential functions were examined by site-directed mutagenesis. Based on kinetic data of various site-directed PPDC variants and by comparison to 3D structures of PDC and benzoylformate decarboxylase, a model of the active site was generated. As in most other ThDP-dependent enzymes a glutamate residue (Glu-48 of PPDC) appears to be responsible for ThDP activation. Residues Ser-25, His-110, and Asp-297 affect the catalytic activity and are probably located in the direct vicinity of the substrate binding site. Residues Asp-265, Asn-293, and Gly-294 were found within the conserved ThDP-binding motif and mark the binding site of the Me^{2+} ion that is responsible for ThDP anchoring. Asp-263 is conserved in PPDC sequences and in sulfopyruvate decarboxylase, and appears to contribute to the metal ion binding site, too. Glu-224, another conserved residue is essential for catalytic activity. The results for Glu-224 and Asp-263 are contrary to the description of the corresponding residues in the PPDC of the gram-negative bacterium *Bacteroides fragilis* [G. Zhang, J. Dai, Z. Lu, D. Dunaway-Mariano, J. Biol. Chem. 278 (2003) 41302–41308].

1. Introduction

Thiamine diphosphate (ThDP) cofactor-dependent enzymes perform a variety of reactions, including oxidative or non-oxidative decarboxylation of α-keto acids, carboligations or group transfer reactions (for reviews see [1–7]). Several ThDP enzymes are in use for biocatalytic purposes [1–3]. Comparisons of available X-ray structures of enzymes as well as structure predictions have revealed that these enzymes can be classified by their domain architecture [4–9]. Domains which are common to all ThDP enzymes are the pyrophosphate (PP) and the pyrimidine binding (Pyr) domain. Additional domains occur, e.g. TKC for transketolase C-terminal domain or TH3 domain in pyruvate decarboxylase (PDC). Thereof, six groups of enzymes are inferred based on domain arrangement [4,5]. Most well-studied ThDP enzymes consist of more than two domains in one contiguous polypeptide. The PP- and Pyr-domains are discussed to have diverged from a common ancestor and then fused into a single chain [5,8]. Thus, sulfopyruvate decarboxylase (SPDC) most closely resembles the unfused ancestor as it consists of an alpha and a beta subunit which correspond to the Pyr and PP domains, respectively. Phosphonopyruvate decarboxylase is structurally closest to the fused common ancestor as discussed recently [4,5]. Analysis of its structure may

* Corresponding author. Present address: Institut für Mikrobiologie, Universität Stuttgart, Allmandring 31, D-70569 Stuttgart, Germany. Tel.: +49 711 685 65487; fax: +49 711 685 65725.
E-mail addresses: g.sprenger@imb.uni-stuttgart.de, georg.sprenger@imb.uni-stuttgart.de (G.A. Sprenger).
[1] Present address: IZKF Biomat, Universitätsaugenklinik, RWTH Aachen, Pauwelsstraße 30, D-52074 Aachen, Germany.

1381-1177/$ – see front matter © 2009 Elsevier B.V. All rights reserved.
doi:10.1016/j.molcatb.2009.03.016

therefore be of general interest to study the evolution of ThDP enzymes.

Phosphonopyruvate decarboxylase (PPDC) enzymes are involved in the biosynthesis of various organophosphonates in bacteria such as actinomycetes which produce phosphonates that are in use either as antibiotics (fosfomycin), or herbicides such as glyphosate or phosphinothricine (bialaphos) [10–12]. Phosphonates are compounds with a stable, covalent carbon to phosphorus (C–P) bond that makes these compounds resistant against chemical hydrolysis, thermal decomposition and photolysis [13]. Apart from antibiotics and herbicides, phosphonates are being used as anti-metabolites or as substrate analogue inhibitors for the determination of enzyme active sites [14]. Biosynthesis of natural phosphonate compounds starts by a rearrangement from phospho*enol*pyruvate (PEP) to phosphonopyruvate (PnPyr) via the enzyme PEP phosphomutase (Ppm). This reaction has an equilibrium which strongly prefers PEP formation [15]. PPDC catalyses the ThDP-dependent decarboxylation of phosphonopyruvate [10] to phosphonoacetaldehyde (PnAA, the precursor for most natural C–P-compounds) and thus irreversibly withdraws the C–P bond from the equilibrium and ensuring forward commitment of the whole pathway [15]. PPDC genes have been originally detected in various streptomycetes [10,11,16–18]. A biochemical and genetical characterization of the PPDC enzyme which is involved in the biosynthesis of the cell wall compound aminoethylphosphonate (AEP) of the gram-negative *Bacteroides fragilis* [15] has been given recently. So far, however, no X-ray structure of PPDC is available. Here we present the recombinant production and biochemical characterization of PPDC from the actinomycete *Streptomyces viridochromogenes* Tü494 [11] in *Escherichia coli* strains. Furthermore, we used site-directed mutagenesis in order to understand the role of essential amino acid residues of the enzyme in comparison with the structure model of the related ThDP enzyme, pyruvate decarboxylase (PDC).

2. Results and discussion

2.1. Cloning and recombinant expression of PPDC from Streptomyces viridochromogenes Tü494

Cloning and sequence analysis of the PPDC encoding gene (*ppd*) from *S. viridochromogenes* Tü494, a producer of phosphinothricin tripeptide (bialaphos) has first been reported by the group of Wohlleben and co-workers [11]. The derived *ppd* protein sequence comprises 397 amino acids. A pairwise sequence alignment with the phosphonopyruvate decarboxylases from *S. hygroscopicus* [10,16] and *S. wedmorensis* [17,18] which are involved in the biosynthesis of bialaphos and fosfomycin, gave 74 and 39% sequence identities, respectively. A sequence alignment with the Ppd from the AEP-producing strain *B. fragilis* [15] showed a sequence identity of 33%.

The *ppd* gene from plasmid pDS 55 [11] was subconed and PCR-modified to encode an amino-terminal 10-fold histidine-tagged PPDC protein (see Section 3 for details). The protein was overexpressed in a recombinant *E. coli* BL21(DE3)/pLysS strain and purified to homogeneity (Fig. 1) by nickel affinity chromatography, resulting in the isolation of about 15 mg of pure protein per liter of liquid culture.

The theoretical molecular weight of the histidine-tagged PPDC calculated from the amino acid sequence was 43,600 Da. The subunit size estimated by SDS–PAGE analysis was around 46,000 Da (Fig. 1). Gel filtration chromatography indicated an apparent molecular mass of 72,100 ± 220 Da. Thus, the quaternary structure of the PPDC appears to be homodimeric. For the PPDC from *B. fragilis*, a homotrimeric structure has been suggested [15].

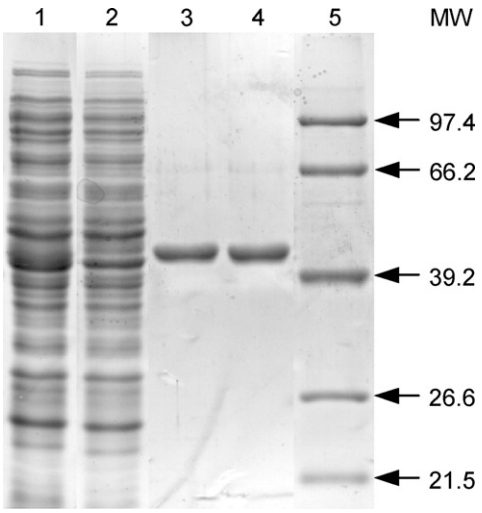

Fig. 1. Coomassie blue-stained SDS–PAGE of the recombinant amino-terminal 10-fold histidine-tagged *S. viridochromogenes* Tü494 PPDC isolated at each stage of Ni-NTA purification procedure. Lane 1, crude extract of the recombinant *E. coli* expression strain; lane 2, Ni-NTA flow-through of the unbound proteins; lanes 3 and 4, fractions of the eluted PPDC protein; lane 5, protein size standards (in kDa).

2.2. Enzyme assays and biochemical characterization of PPDC

2.2.1. Enzyme assays

The substrate of PPDC, phosphonopyruvate (PnPyr), was not commercially available. PPyr was synthesized according to established methods ([19,20], see Section 3) by A. Cosp, L. Walter, and M. Müller at the Institute of Biotechnology 2 at the Forschungszentrum Jülich. The PPDC catalyzed decarboxylation of PnPyr to phosphonoacetaldehyde (PnAA) can be directly followed by HPLC and MS (data not shown). As this method was not suitable for routine assays, two coupled reactions with auxiliary enzymes were established. One used the auxiliary enzyme phosphonoacetaldehyde phosphonatase (Phtase) from *Pseudomonas putida* KT 2440, which was prepared in a His-tagged recombinant form and used to convert phosphonoacetaldehyde (PnAA; the product of PPDC reaction) to acetaldehyde, which was then assayed by alcohol dehydrogenase (ADH) and the concomitant oxidation of NADH. Secondly, PnAA was converted to 2-aminoethylphosphonate by *P. putida* KT 2440 aminoethylphosphonate aminotransferase (AEPT; prepared in a recombinant His-tagged form from *E. coli* BL21) with the concomitant conversion of L-alanine to pyruvate which was detected by lactate dehydrogenase (LDH) as additional auxiliary enzymes. The principle reactions are given in Fig. 2. Direct comparison of both enzyme assays gave very good concordance in activity.

2.2.2. pH and temperature dependence of catalysis

The pH rate profile followed a bell-shaped curve and defined pH 7.5–8.5 as the pH range for optimal PPDC catalysis, whereas the used buffer systems had no influence on the catalytic activity. Analysis of the temperature profile revealed an activation energy of about 45 kJ/mol, which is a typical value for enzyme activation energies [21]. Storage at −20 °C and 4 °C yielded in a half-life of about 50 days.

2.2.3. Kinetic characterization of phosphonopyruvate decarboxylase

Using the two different coupled enzyme assays Phtase/ADH and AEPT/LDH (see Sections 2.2.1 and 3) at a pH of 8.0 and a temperature of 30 °C, PPDC reaction followed Michaelis–Menten kinetics with phosphonopyruvate, yielding a K_m value of 3.2 ± 0.35 μM (which is in the same range as the K_m value determined earlier for the PPDC

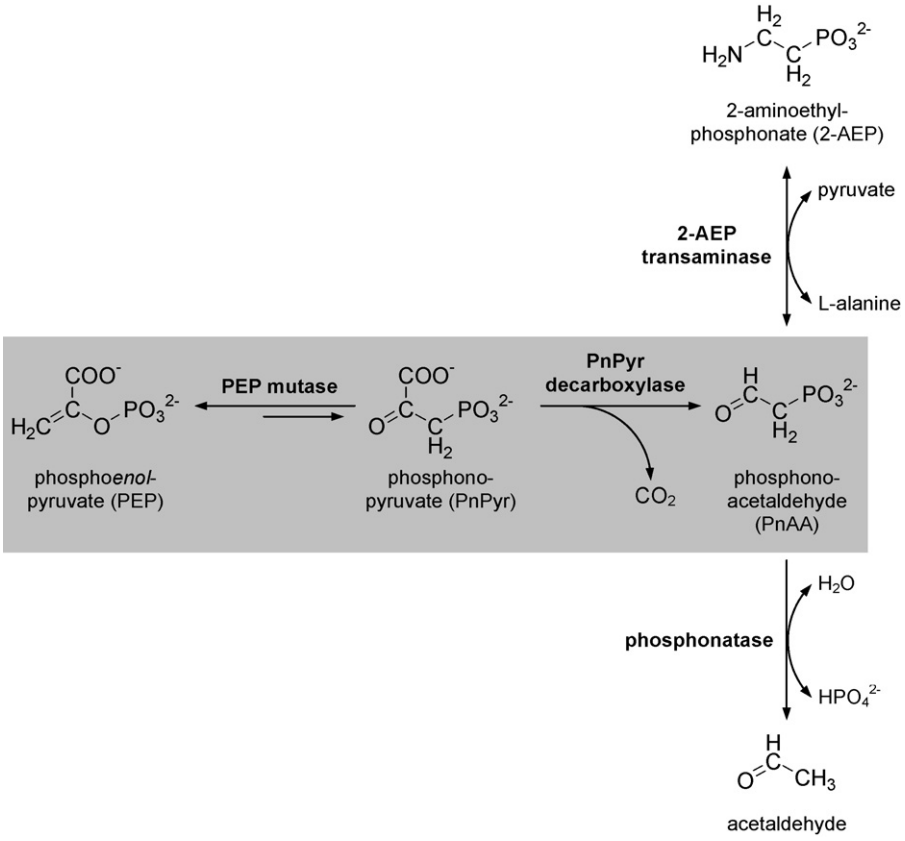

Fig. 2. Enzymatic reactions from phospho*enol*pyruvate (PEP) to phosphonoacetaldehyde (PnAA) via rearrangement to phosphonopyruvate (PnPyr) and principle of coupled PPDC enzyme assays using 2-aminoethylphosphonate (2-AEP) transaminase and phosphonatase. Acetaldehyde can be assayed by alcohol dehydrogenase and the concomitant oxidation of NADH. AEP formation from PnAA can be measured via the concomitant conversion of L-alanine to pyruvate and the following NADH-coupled reduction of pyruvate to lactate by lactate dehydrogenase.

from *B. fragilis* [15]), a k_{cat} value of $1.2 \pm 0.02\ s^{-1}$, and a k_{cat}/K_m value of $3.8 \times 10^5\ s^{-1}\ M^{-1}$.

Neither pyruvic acid, nor β-hydroxypyruvic acid or β-fluoropyruvic acid were converted by the PPDC of *S. viridochromogenes* to the respective aldehydes (data not shown). This is in accordance with the findings of Zhang et al. [15] who assumed that, in the case of the *B. fragilis* PPDC, the C–P and not the carboxyl group, is essential in substrate binding. As the structure analogue, sulfopyruvate, was not available, it could not be tested as a potential substrate for PPDC.

2.2.4. Metal ion and ThDP activation

ThDP- and metal ion-free apo-PPDC, prepared by exhaustive dialysis, showed a drastically decreased residual activity (<2%). Subsequent addition of 1 mM ThDP and Mg^{2+} (final concentrations) resulted in a partial reconstitution of activity (45%). Besides Mg^{2+}, the metal ions Ca^{2+}, Mn^{2+}, Co^{2+}, Ni^{2+}, and Zn^{2+} were tested as potential activators of the metal-free PPDC in the presence of 1 mM ThDP and saturating phosphonopyruvate (0.5 mM). Only Ca^{2+} and Mn^{2+} were used as activators. Whereas the k_{cat} values of the Mg^{2+}-, Ca^{2+}-, and Mn^{2+}-activated Ppd were in the same range (0.52–0.85 s^{-1}), the K_m value for Mn^{2+} (~3 μM) was significantly lower than the K_m values for Mg^{2+} and Ca^{2+} (~40 μM). These results were in accordance with those obtained with the *B. fragilis* PPDC [15]. The K_m value for ThDP activation was determined by measuring the catalytic activity of the 1 mM Mg^{2+}-activated PPDC in the presence of saturating phosphonopyruvate (0.5 mM). The data defined a k_{cat} value of 0.55 s^{-1} and a K_m value of about 39 μM (Table 1). In the case of the *B. fragilis* PPDC the K_m value for ThDP was of about 13 μM [15], whereas other ThDP-activated enzymes have been reported to bind ThDP with K_m values in the nanomolar to micromolar range [22–26].

2.3. PPDC sequences in comparison to other ThDP enzymes

PPDC, as well as sulfopyruvate decarboxylase [27] belongs to a family of ThDP- and Me^{2+}-dependent decarboxylases, which catalyze the decarboxylation of an α-keto carboxylate using ThDP as an "electron sink" [15]. This enzyme family includes acetohydroxyacid synthase [28–30], acetolactate synthase [31], benzoylformate decarboxylase (BFD) [32–34], glyoxylate carboligase [35–36], indole pyruvate decarboxylase [24,37,38], pyruvate decarboxylase (PDC) [22,39,40], and pyruvate oxidase [41–43].

Members of an enzyme superfamily, which catalyze different overall reactions, share a common structural scaffold and retain crucial catalytic amino acid residues [44]. Together with site-directed mutagenesis, the knowledge of three-dimensional structures of

Table 1
Metal ion and ThDP dependence of steady-state kinetic constants.

Cofactor	K_m [μM]	k_{cat} [s^{-1}]
Mg^{2+}	38.91 ± 1.46	0.52 ± 0.008
Ca^{2+}	36.57 ± 4.47	0.66 ± 0.014
Mn^{2+}	2.88 ± 0.27	0.85 ± 0.012
ThDP	39.05 ± 2.64	0.55 ± 0.003

The metal ion dependence of the steady-state kinetic constants for PPDC catalysis was measured in the presence of saturating phosphonopyruvate (0.5 mM) and ThDP (1 mM) at pH 8.0 and 30 °C. Co^{2+}, Ni^{2+}, and Mn^{2+} were no activators. The ThDP dependence of the steady-state kinetic constants for PPDC catalysis was measured in the presence of saturating phosphonopyruvate (0.5 mM) and Mg^{2+} (1 mM) at pH 8.0 and 30 °C.

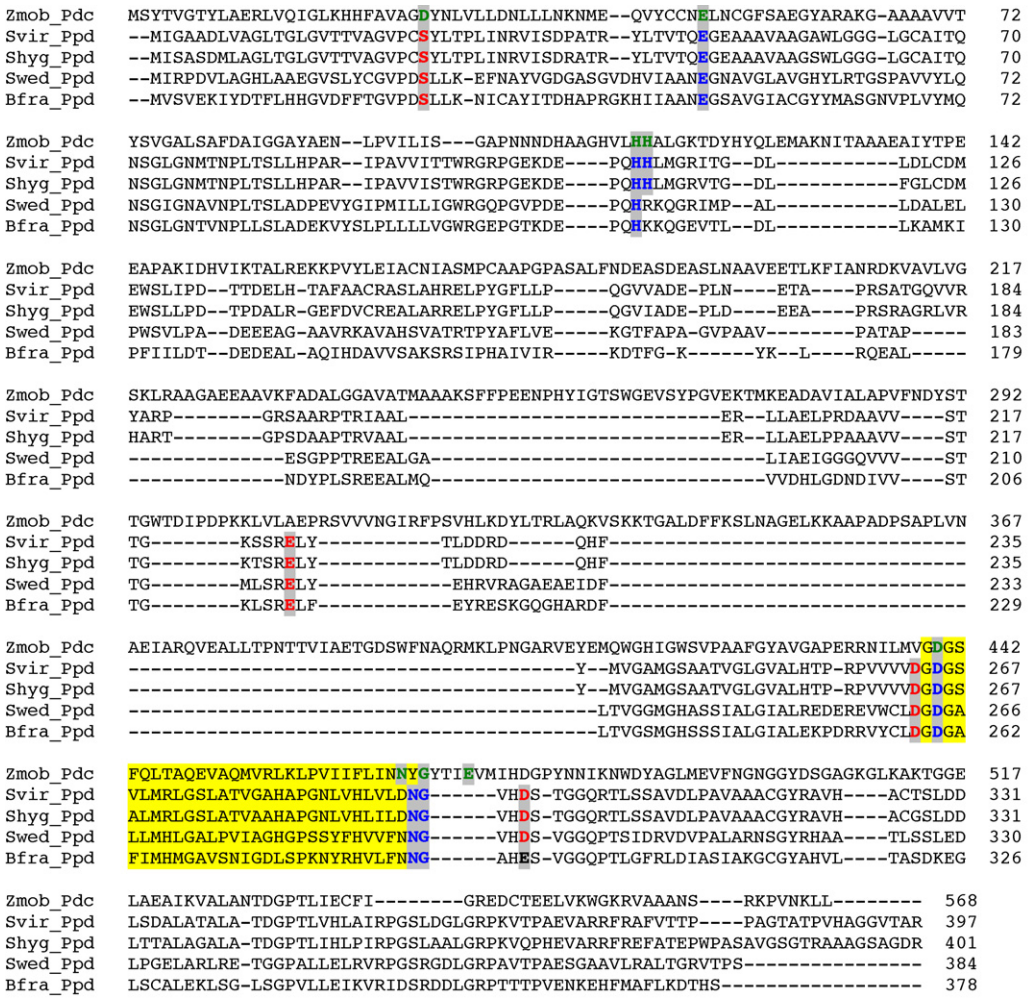

Fig. 3. Sequence alignment of phosphonopyruvate decarboxylases from *S. viridochromogenes*, *S. hygroscopicus*, *S. wedmorensis*, and *B. fragilis* in comparison with the sequence of pyruvate decarboxylase from *Z. mobilis*. Conserved PPDC amino acid residues, which were identified by means of the *Z. mobilis* PDC (printed in green and highlighted in grey), are printed in blue and highlighted in grey. The red printed and grey highlighted amino acid residues serine (S), glutamate (E) and aspartate (D) are conserved amino acid residues in all PPDC sequences and are not found in *Z. mobilis* PDC sequence. The ThDP signature motif is highlighted in yellow. Zmob_Pdc, *Z. mobilis* pyruvate decarboxylase (GenBank accession: CAA42157); Svir_Ppd, *S. viridochromogenes* phosphonopyruvate decarboxylase (GenBank accession: CAA74722); Shyg_Ppd, *S. hygroscopicus* phosphonopyruvate decarboxylase (GenBank accession: BAA07055); Swed_Ppd, *S. wedmorensis* phosphonopyruvate decarboxylase (GenBank accession: BAA32496); Bfra_Ppd, *B. fragilis* phosphonopyruvate decarboxylase (GenBank accession: AAG26466). (For interpretation of the references to color in this figure legend, the reader is referred to the web version of the article.)

various ThDP-dependent decarboxylases [32,39,45–49] allowed the identification of several amino acid residues located at the active site or which are important for catalytic activity, respectively. By means of an alignment of the phosphonopyruvate decarboxylases from *S. viridochromogenes*, *S. hygroscopicus*, *S. wedmorensis*, and *B. fragilis* with the sequence of the well characterized PDC from *Zymomonas mobilis* (Fig. 3) and comparison to the BFD from *P. putida* [32,33], several conserved residues could be identified in the PPDC sequences.

The common step for all ThDP-dependent enzymes is the activation of the nucleophilic C2-atom (located between the nitrogen and sulfur atom in the thiazole ring [50]), that occurs via deprotonation. A conserved glutamate residue donates a hydrogen bond to the N1′-atom of the pyrimidine ring of ThDP, resulting in the activation of the C4′-amino group, which is the acceptor of the attached C2–ThDP–proton [51]. In PPDC sequences, the strictly conserved glutamate residue Glu-48 (E48; in *S. viridochromogenes* PPDC numbering), was identified and predicted to be necessary for ThDP activation. We generated the variant E48 > Q by site-directed mutagenesis (see Section 3). This variant was found to be expressed to nearly the same extent as the wt-PPDC but showed no detectable activity. This result is in accordance with this residue's assumed function in carbanion formation (Fig. 4).

The amino acid sequence glycine–aspartate–glycine and two asparagine which are about 25 amino acid residues apart, have been recognized in several ThDP enzymes [52,53] and was later on proposed as ThDP-binding motif [53]. From several 3D structures of ThDP-dependent enzymes it had become apparent that a divalent metal ion functions to anchor the ThDP molecule by coordinating to two of the diphosphate oxygen atoms, to the side chain oxygen atoms of the aspartate- and the second asparagine-residue of the ThDP-binding motif, and to the main chain oxygen atom of a glycine-residue that is directly located behind the ThDP-binding motif [46]. In *S. viridochromogenes* PPDC the ThDP-binding motif is likely to stretch from G264–D265–G266 to N293–G294. The amino acid residues D265, N293 and G294 were identified as potential candidates for binding and anchoring the cofactors. To test their respective contributions to catalysis, the variants D265A, N293A, and G294A were prepared. In the presence of 1 mM Mg^{2+} the variants D265A and N293A showed no detectable activity. These results are consistent with the assignment of the ThDP-binding motif in the phosphonopyruvate decarboxylases as indicated in Figs. 3 and 4.

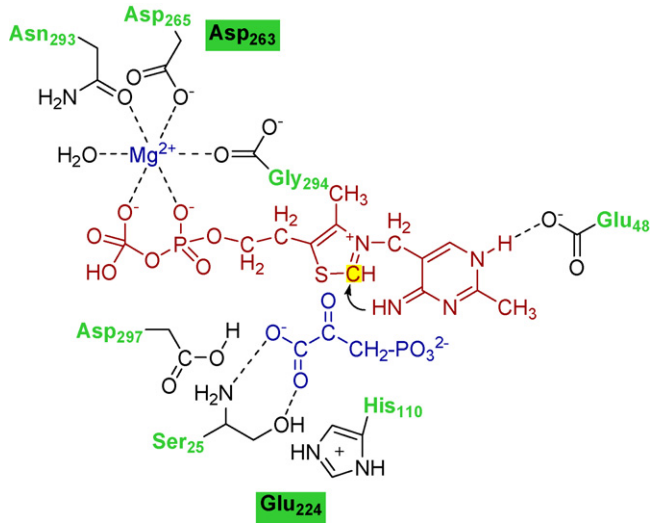

Fig. 4. Hypothetical two-dimensional model of the active site of *S. viridochromogenes* PPDC based on data of PDC (according to Candy and Duggleby [55], Polovnikova et al. [33], and Tittmann et al. [58] and mutagenesis data of the present work. The scheme displays the starting point of the reaction cycle, which is initiated by the deprotonation of the nucleophilic C2-atom (highlighted in yellow) in the thiazole ring of ThDP (printed in red). The putative interactions of essential amino acid residues (printed in green) with both cofactors (ThDP and Mg^{2+} (printed in blue)) and with the substrate phosphonopyruvate (printed in blue) are drawn as dashed lines. Putative positions of glutamate-224 and aspartate-263 are highlighted in green. (For interpretation of the references to color in this figure legend, the reader is referred to the web version of the article.)

Interestingly, in the case of D265A, the addition of 1 mM Mn^{2+} resulted in a restoration of activity (30% of wt-PPDC). This may reflect the higher affinity of PPDC to Mn^{2+} relative to other divalent metal ions.

The steady-state kinetic constants of the variant G294A were determined to be $K_m = 6.2 \pm 2.35\ \mu M$ and $k_{cat} = 0.29 \pm 0.01\ s^{-1}$. Compared to wt-PPDC, K_m is increased only twofold, while k_{cat} is fourfold lower. Thus, the substrate affinity is less affected than the catalytic activity which is in line with the assumption that glycine-294 belongs to the cofactor-binding and -anchoring amino acid residues (Fig. 4).

The 3D structure of the *Z. mobilis* PDC shows that the cofactor-bound substrate and the cofactor-bound product are surrounded by the mostly conserved amino acid residues aspartate-27, histidine-113, histidine-114, and glutamate-473 [46]. The importance of D27, H113, H114, and H114 in PDC catalysis was approved by site-directed mutagenesis [54–57]. While H114 is assigned to orientate a catalytic intermediate, H113 and D27 affect the acetaldehyde release [58]. D27 is conserved in pyruvate and indole pyruvate decarboxylases. In BFD, the amino acid at this position is a serine residue, proposed to donate a hydrogen bond to the carboxylate group of the substrate [32]. In the PPDC sequences, a conserved serine residue (S25; in *S. viridochromogenes* PPDC numbering) was found as well. In order to check the function of S25, the variants S25D and S25N were prepared. Their steady-state kinetic constants are listed in Table 2. In the case of S25N, catalytic turnover rate is 1.5-fold less compared to the wt-PPDC and K_m is increased 80-fold, whereas catalytic turnover rate of S25D is 4-fold less and K_m is increased 460-fold. The results showed, that in PPDC the uncharged polar amino acid residue S25 is important to substrate binding (Fig. 4). The histidine doublet typical for PDCs was also found in the PPDC sequences of *S. viridochromogenes* and *S. hygroscopicus* (H110 and H111) (Fig. 3). The variants H110A and H111A were prepared to assess the degree to which H110 and H111 contribute to PPDC catalysis. The variant H110A showed no detectable activity, whereas the exchange of histidine-111 to alanine had no significant influence on the steady state kinetic constants (Table 2). While H110 is especially important for catalysis (illustrated in Fig. 4), the possible function of H111 in orientating a catalytic intermediate is therefore questionable. It cannot be ruled out that a more distant histidine residue may contribute to PPDC catalysis, as it was reported for BFD [32] and transketolase [59]. In *Z. mobilis* PDC, E473 plays an important role in substrate orientation during covalent substrate binding and in stereochemical control of the decarboxylation step [60]. In the case of the *Streptomyces* PPDC sequences a conserved aspartate residue (D297) was recognized (Fig. 3). Thus, the variants D297E and D297N were prepared. Their steady-state kinetic constants are listed in Table 2. In the case of D297E, catalytic turnover rate is 1.5-fold less compared to the wt-PPDC and K_m is increased about 13-fold, whereas catalytic turnover rate of D297N is twofold lower and K_m is increased 940-fold. The results show, that together with S25, the negatively charged amino acid residue D297 is especially important to substrate binding (Fig. 4).

Table 2
Steady-state kinetic constants of wt-PPDC and PPDC variants.

Enzyme	K_m [μM]	k_{cat} [s^{-1}]
wt-PPDC	3.2 ± 0.35	1.18 ± 0.02
S25D	1470 ± 180	0.31 ± 0.01
S25N	250 ± 20	0.78 ± 0.01
H111A	13 ± 0.01	1.24 ± 0.09
D297E	40 ± 10	0.76 ± 0.01
D297N	3020 ± 110	0.55 ± 0.02

The steady-state kinetic constants of wt-PPDC and PPDC variants catalyzing decarboxylation of phosphonopyruvate was measured in the presence of 1 mM ThDP and 1 mM Mg^{2+}, at pH 8.0 and 30 °C.

2.4. Amino acid residues unique to the phosphonopyruvate and sulfopyruvate decarboxylases

By means of a comparison of all published PPDC sequences plus an alignment with the sulfopyruvate decarboxylase, Zhang et al. [15] had identified 12 polar amino acid residues conserved in the protein sequences of the phosphonopyruvate and sulfopyruvate decarboxylases. Site-directed mutagenesis of two amino acid residues belonging to this group (glutamate-213 and aspartate-258) revealed, that E213 does not appear to play an important role in PPDC catalysis, whereas D258 is especially important to substrate binding [15]. To examine, whether the corresponding residues glutamate-224 and aspartate-263 of *S. viridochromogenes* PPDC (Fig. 3) have the same functions, the variants E224A and D263A were prepared. However, in the presence of 1 mM Mg^{2+} both variants showed no detectable activity. As described for D265A, the presence of 1 mM Mn^{2+} resulted in an increased activity of D263A (20% of the wt-PPDC value). Because of the position of D263 (located immediately in front of the ThDP binding motif) and of the consistent behavior of D263A and D265A in the presence of 1 mM Mn^{2+} aspartate-263 could be located close to the metal ion binding site and therefore affect the binding of the bivalent metal ion (Fig. 4). In contrast to D263A, the presence of 1 mM Mn^{2+} could not enhance activity of E224A. If E224 is located within the active site and nearby the substrate binding site, respectively, this glutamate residue is possibly important to PPDC catalysis (Fig. 4).

The postulated functions of E224 and D263 are in contradiction to the findings of the corresponding residues of the *B. fragilis* PPDC [15]. Together with the different oligomerization states of the native proteins this points to likely differences in the 3D structures of *S. viridochromogenes* and *B. fragilis* PPDC enzymes.

2.4.1. Concluding remarks

In the absence of a 3D structure of any phosphonopyruvate decarboxylase, we have compared various PPDC sequences, both

by sequence alignment and by analogy to the related *Z. mobilis* PDC, for which a 3D structure is available. Site-directed mutagenesis of residues which were proposed to interact with ThDP or metal ion binding was performed. Analysis of these variants let us propose a mechanism given in Fig. 4 highlighting residues which are likely to interact with the cofactors and possibly (serine-25 and aspartate-297) with the substrate, phosphonopyruvate. Differences to the *B. fragilis* PPDC became apparent (oligomerization state, role of various amino acid residues).

3. Experimental

3.1. Materials

Thiamine diphosphate chloride (ThDP) was purchased from Sigma–Aldrich. Dihydro-β-nicotinamide adenine dinucleotide (NADH), yeast alcohol dehydrogenase (ADH), hog muscle L-lactate dehydrogenase (LDH), and enzymes used in DNA manipulation were purchased from Roche Diagnostics, Mannheim, Germany. Other chemicals were from commercial origin and at the highest available purity. Phosphonopyruvate was synthesized according to published methods [19,20] and were a gift from A. Cosp, L. Walter, and M. Müller (Institute of Biotechnology 2, Forschungszentrum Jülich, Germany).

3.2. PCR-amplification and cloning of the genes ppd, phnW and phnX

Recombinant *S. viridochromogenes* Tü494 phosphonopyruvate decarboxylase (PPDC), recombinant *P. putida* KT2440 2-aminoethylphosphonate transaminase (AEPT) and phosphonoacetaldehyde hydrolase (Phtase) were purified as fusion proteins with amino-terminal 10-fold histidine-tags. For PCR amplification and cloning of PPDC, the *ppd* gene was amplified by using the primers 5′ to 3′ CGGTGCACATATGATCGGCGCGGC and 3′ to 5′ ATCTGCTCGAGGCTCATCGTGCGGTC with engineered restriction sites underlined. For PCR amplification and cloning of the *phnW* gene (AEPT) the sequences of primers were 5′ to 3′ GTGAGGAATAACCATATGAGCAACGCCCCG and 3′ to 5′ TTCGGCTCGAGAAAGCGTCAGATATCCAGC, and for the *phnX* gene (Phtase), the sequences of primers were 5′ to 3′ GAGTTAGCGCATATGAACTACAACAACCCC and 3′ to 5′ GAAACCTCGAGGGTCAGAAGGCTTGCGG. All primers used in DNA manipulation, DNA sequencing, or site-directed mutagenesis were custom synthesized at MWG Biotech, Ebersberg, Germany.

For amplification of the *S. viridochromogenes* Tü494 *ppd* gene, the plasmid pJF119*ppd*bgl was used as DNA template. pJF119*ppd*bgl had been constructed by ligating a *Bgl*II/*Nru*I fragment containing the *ppd* gene on plasmid pDS55 (Wohlleben, W., University of Tübingen, unpublished) into the vector pJF119EH [61], which had been restricted with BamHI and HindIII (blunted). DNA template was denatured for 3 min at 95 °C. The *ppd* gene was amplified by 10 cycles of 95 °C denaturation for 30 s, 68 °C annealing for 30 s, 72 °C elongation for 70 s, 30 cycles of 95 °C denaturation for 30 s, 68 °C annealing for 30 s, 72 °C elongation for 70 s plus 5 s per cycle, and a final 72 °C elongation for 7 min using the GC-Rich PCR System (Roche). For amplification of the genes *phnW* and *phnX*, genomic DNA from *P. putida* KT2440 [62] was used as template. In an initial step, DNA template was denatured (2 min at 94 °C). The *phnW* gene was amplified by 10 cycles of 94 °C denaturation for 15 s, 67 °C annealing for 30 s, 72 °C elongation for 50 s, 17 cycles of 94 °C denaturation for 15 s, 67 °C annealing for 30 s, 72 °C elongation for 50 s plus 3 s per cycle, and a final 72 °C elongation for 7 min using the *Pwo* DNA polymerase (Roche). The *phnX* gene was amplified by 10 cycles of 94 °C denaturation for 15 s, 66.5 °C annealing for 30 s, 72 °C elongation for 45 s, 17 cycles of 94 °C denaturation for 15 s, 66.5 °C annealing for 30 s, 72 °C elongation for 45 s plus 3 s per cycle, and a final 72 °C elongation for 7 min using the *Pwo* DNA polymerase (Roche). The PCR products were purified by gel electrophoresis and digested using NdeI and XhoI restriction enzymes. The digest was ligated to an NdeI- and XhoI-cut pET-16b vector (Novagen). After transformation into *E. coli* DH5α the integrity of the resulting plasmids was checked by restriction analysis and DNA sequencing. In the case of PPDC, possible amino acid changes at the positions 316 and 317 were adjusted by site-directed mutagenesis using the QuickChange Site-Directed Mutagenesis Kit (Stratagene), simultaneously generating a PstI restriction site at the position 944–949. The primer sequence was 5′-CCCGCCGTCGCtGCaGCCTGCGGCTACCG-3′, where the lower case letters represent the mismatches to the wild-type (wt-) sequence and the underlined sequence is the newly incorporated *Pst*I restriction site. The resulting expression vectors, named pET16*ppd*A337-339, pET16aept and pET16phtase, respectively, were used to transform *E. coli* BL21(DE3)pLysS competent cells.

3.3. Site-directed mutagenesis of ppd gene

The site-directed PPDC variants S25D and S25N (nucleotides (nt) 73–75), E48Q (nt 142–144), H110A (nt 328–330), H111A (nt 331–333), E224A (nt 670–672), D263A (nt 787–789), D265A (nt 793–795), N293A (nt 877–879), G294A (nt 880–882), D297E and D297N (nt 889–891) were prepared by PCR using the QuickChange Site-Directed Mutagenesis Kit (Stratagene) according to manufacturer's directions with the expression vector pET16ppdA337-339 used as DNA template. For generation of the PPDC variants, the primer sequences were 5′-GCCGGAGTGCCCTGCgaCTACCTGACCCCG-3′ for S25D, 5′-CGTGGCCGGAGTGCCCTGCaaCTACCTGACCCCGTTGATCAACC-3′ for S25N, 5′-CCTCACGGTCACGCAGcAGGGCGAGGCCGC-3′ for E48Q, 5′-GGACGAGCCCCAGgcC CACCTGATGGGCCGG-3′ for H110A, 5′-CGAGCCCCAGC ACgcCCTGATGGGCCGGATCA CC-3′ for H111A, 5′-GGCAAGTCCAGCCGGGcGCTGTACACCCTCG-3′ for E224A, 5′-CCGCCCGGTCGTGGTCGTCGcaGGCGACGGCTCGGTGCTGATGCG-3′ for D263A, 5′-GTCGTGGTCGTCGACGGCGcaGGCTCGGTGCTGATG-3′ for D265A, 5′-CCACCTGGTCC TCGACgcaGGCGTCCACGACTCC-3′ for N293A, 5′-CCTGGTCCTCGACAACGcCGTCCAC GACTCCACC-3′ for G294A, 5′-CGACAACGGCGTCCACGAaTCCACCGGCGGCCAGC-3′ for D297E, and 5′-CGACAACGGCGTCCACaACTCCACCGGCGGCCAGC-3′ for D297N, whereas the lower case letters represent the mismatches to the wild type sequence. The gene sequences were verified by DNA sequencing. The variants were prepared in the same manner as the wt-PPDC. The expression rates were between 10 and 15 mg mutant protein/l.

DNA sequencing was performed with LI-COR 4200 (MWG Biotech) using the Thermo Sequenase fluorescent labelled primer cycle sequencing kit with 7-deaza-dGTP (Amersham Biosciences) and the IRD-800 labeled primers T7promotor (5′-TAATACGACTCACTATAGGG-3′) and T7terminator (5′-GCTAGTTATTGCTCAGCGG-3′). In case of the *ppd* gene two additional IRD-800 labeled primers were used: 5′-AGGACAGGTCGTACGGTACGC-3′ (nt 537–557) and 5′-CATGTAGAAGTGCTGGTCGC-3′ (nt 711–692). Computer analysis of the sequences was performed using the Base ImagIR 4.1 software package.

3.4. Protein purification

E. coli BL21(DE3)pLysS cells, carrying the according expression vector, were grown aerobically in 6× 400 ml Luria–Bertani medium [63] containing 100 μg/ml ampicillin and 34 μg/ml chloramphenicol

col. After cultivation at 37 °C for 75 min, the incubation temperature was lowered to 30 °C. Induction of protein expression with a final concentration of 0.5 mM isopropyl-β-D-thiogalactopyranoside was performed when an optical density (OD_{600}) of 0.8–1.0 had been reached. After 5 h, cells were harvested by centrifugation for 10 min at 6000 × *g* and 4 °C, washed and resuspended in 20 ml of the respective washing buffer (PPDC: 20 mM HEPES, 300 mM NaCl, 20 mM imidazole, 1 mM ThDP, 2 mM $MgCl_2$ and 1 mM dithiothreitol (DTT), pH 7,5; AEPT: 10 mM KH_2PO_4, 20 mM imidazole, 10 μM pyridoxal phosphate (PLP) and 1 mM DTT, pH 7.5; Phtase: 50 mM HEPES, 20 mM imidazole, 10 mM $MgCl_2$ and 1 mM DTT, pH 7,5) and stored at −80 °C for at least 12 h. Thawing the cells at 25 °C resulted in cell lysis. After storage on ice for 1 h and centrifugation for 1 h at 48,000 × *g* and 4 °C, the supernatants were used as cell-free extracts. The cell-free extracts were applied to a 25 ml bed volume Ni-NTA Superflow column (Qiagen) equilibrated with 3–4 column volumes of the respective washing buffer, which were also used to remove unbound proteins from the column. In the case of PPDC, unspecific bound proteins were eluted with buffer containing 80 mM imidazole. The elution of the His-tagged proteins was achieved with buffer containing 250 mM imidazole. After protein elution a desalting step was performed to remove imidazole using Centriprep YM-30 devices (Millipore) and the respective storage buffer (PPDC: 50 mM HEPES, 300 mM NaCl, 1 mM ThDP, 1 mM $MgCl_2$ and 1 mM DTT, pH 8.0; AEPT: 50 mM TRICINE, 100 μM PLP and 1 mM DTT, pH 8.5; Phtase: 50 mM HEPES, 300 mM NaCl, 10 mM $MgCl_2$ and 1 mM DTT, pH 8.0). The obtained fusion protein yields were 15 mg PPDC/l; 30 mg AEPT/l; 90 mg Phtase/l, which were stored at 4 °C.

The molecular masses were calculated from the amino acid composition using the EXPASY Molecular Biology Server program Compute pI/MW [64] and measured by SDS–PAGE (6% stacking gel and 12% separating gel). The size of the native PPDC protein was estimated by gel filtration column chromatography using the column HiLoad 26/60 Superdex 200 prep grade (Amersham Biosciences) at a flow rate of 2.5 ml/min and the eluent 20 mM HEPES, 300 mM NaCl, and 1 mM DTT, pH 8.0. The column was calibrated using the standard proteins α-amylase (200 kDa), ADH (150 kDa), albumin (66 kDa), carbonic anhydrase (29 kDa), and cytochrome C (12.4 kDa) and void volume was determined using blue dextran. Protein concentration was determined according to Bradford [65] using bovine serum albumin for calibration.

3.5. Assays of enzymatic activity

PPDC activity was determined in two different coupled enzyme assays at 30 °C. The rate of phosphonoacetaldehyde production from phosphonopyruvate (PnPyr) was assayed by measuring the oxidation of NADH in the presence of Phtase/ADH and AEPT/LDH, respectively. The conversion of phosphonoacetaldehyde via acetaldehyde (Fig. 2) into ethanol was monitored at 340 nm ($\varepsilon = 6.3\ cm^2/\mu mol$) using 1 ml reaction mixtures containing 0.5 mM PnPyr, 0.3 mM NADH, 100 μg Phtase, and 10 units of ADH in PPDC storage buffer. The conversion of phosphonoacetaldehyde to 2-aminoethylphosphonate (Fig. 2) is coupled to the formation of lactate which was monitored using 1 ml reaction mixtures containing 0.5 mM PnPyr, 2 mM L-alanine, 0.3 mM NADH, 10 μM PLP, 50 μg AEPT, and 11 units of LDH in PPDC storage buffer. The reactions were started by addition of PnPyr. The amount of PPDC was chosen thus that a steady decrease of NADH absorption could be monitored over 5–10 min. One unit is defined as the amount of PPDC that catalyses the decarboxylation of 1 μmol phosphonopyruvate per minute at pH 8.0 and 30 °C. All data points represent the average of at least two independent experiments.

3.6. Enzyme characterization

3.6.1. Steady-state kinetic constant determination

K_m and v_{max} values for the catalytic activity of the wt-PPDC and the PPDC variants were determined from the specific activity data measured as a function of varying phosphonopyruvate concentrations. The k_{cat} value was calculated from v_{max} and the enzyme concentration using the equation $k_{cat} = v_{max}/[E]$.

3.6.2. Metal ion and ThDP activation

Cofactor-free PPDC (apo-PPDC) was prepared by dialysis against a buffer containing 50 mM HEPES, 300 mM NaCl, 10 mM EDTA, and 1 mM DTT, pH 8.0 followed by exhaustive dialysis against a buffer containing 50 mM HEPES, 300 mM NaCl, and 1 mM DTT, pH 8.0 in order to remove EDTA. The rate of phosphonoacetaldehyde production from PnPyr was monitored at 340 nm ($\varepsilon = 6.3\ cm^2/\mu mol$) using the auxiliary enzymes AEPT and LDH. For metal ion activation, 1 ml reaction mixtures contained 0.5 mM phosphonopyruvate, 2 mM L-alanine, 0.3 mM NADH, 1 mM ThDP, 10 μM pyridoxal phosphate (PLP), 100 μg of purified AEPT, 11 units of LDH, and varying concentrations of divalent metal ions in a buffer containing 50 mM HEPES, 300 mM NaCl, and 1 mM DTT, pH 8.0. For ThDP reconstitution, 1 ml reaction mixtures contained 0.5 mM phosphonopyruvate, 2 mM L-alanine, 0.3 mM NADH, 1 mM $MgCl_2$, 10 μM PLP, 100 μg AEPT, 11 units of LDH, and varying concentrations of ThDP. Reactions were started by addition of phosphonopyruvate. The amount of apo-PPDC was chosen in a way that a steady decrease of NADH absorption could be monitored over 10 min. All data points represent the average of at least two independent experiments.

3.6.3. pH-rate profile determination

The effect of pH on the kinetic properties of PPDC was determined using the Phtase/ADH and the Aept/LDH enzyme assay as described above. PPDC activity was measured as a function of the reaction pH by using the following buffer systems at the indicated pH values and at 50 mM concentrations each of either MES (pH 5.5–6.5), MOPS (pH 6.5–7.5), HEPES (pH 7.0–8.0), TRIS (pH 7.0–9.0), BICINE (pH 8.0–9.0), GLYGLY (pH 7.5–9.5), CHES (pH 9.0–10.0), or CAPS (10.0–11.0). Each buffer contained 300 mM NaCl, 1 mM ThDP, 5 mM $MgCl_2$, and 1 mM DTT. Centricon YM-10 devices (Millipore) were used to exchange the PPDC storage buffer. All data points represent the average of at least two independent experiments.

3.6.4. Temperature-rate profile and determination of half-life

The effect of temperature on the kinetic properties of PPDC was determined using the Phtase/ADH and AEPT/LDH enzyme assays as described above. Reaction mixtures were pre-incubated at the respective temperature for 5 min. PPDC activities were determined as a function of the reaction temperature and analyzed using the Arrhenius plot, whereas the activation energy (E_a) was calculated from the resulting slope (k) using the equation $E_a = -k \times R$ ($R = 8.3144\ J/(mol\ K)$). For determination of the half-life ($t_{1/2}$), PPDC was incubated at different temperatures. At several time points the residual enzyme activity was measured by carrying out the Phtase/ADH and the AEPT/LDH enzyme assays as described above. Activity data were plotted as ln(activity) *vs.* incubation time. The half-life was calculated from the resulting slope (k) using the equation $t_{1/2} = \ln 2/k$.

Acknowledgements

We thank Wolfgang Wohlleben (University of Tübingen) for the kind gift of plasmid pDS55 containing the cloned *ppd* gene from *S. viridochromogenes* Tü494. We are especially grateful to A. Cosp, L.

Walter, and M. Müller (Forschungszentrum Jülich, now University of Freiburg) for synthesis of phosphonopyruvate, for help with HPLC and mass spectroscopy and many helpful hints during the work. This work was supported by a grant of the Deutsche Forschungsgemeinschaft through Collaborative Research Center SFB380 (TP B21) to G.S.

References

[1] G.A. Sprenger, M. Pohl, J. Mol. Catal. B: Enzym. 6 (1999) 145–159.
[2] M. Pohl, G.A. Sprenger, M. Müller, Curr. Opin. Biotechnol. 15 (2004) 335–342.
[3] M. Müller, G.A. Sprenger, in: M. Patel, F. Jordan (Eds.), Thiamine: Catalytic mechanisms and Role in Normal and Disease States, Marcel Dekker, Inc., New York, 2003, pp. 77–92.
[4] R.G. Duggleby, Acc. Chem. Res. 39 (2006) 550–557.
[5] S.J. Costelloe, J.M. Ward, P.A. Dalby, J. Mol. Evol. 66 (2008) 36–49.
[6] F. Jordan, Nat. Prod. Rep. 20 (2003) 184–201.
[7] R. Kluger, K. Tittmann, Chem. Rev. 108 (2008) 1797–1833.
[8] A.E. Todd, C.A. Orengo, J.M. Thornton, J. Mol. Biol. 307 (2001) 1113–1143.
[9] Y.A. Muller, Y. Lindqvist, W. Furey, G.E. Schulz, F. Jordan, G. Schneider, Structure 1 (1993) 95–103.
[10] H. Nakashita, K. Watanabe, O. Hara, T. Hidaka, H. Seto, J. Antibiot. (Tokyo) 50 (1997) 212–219.
[11] D. Schwartz, J. Recktenwald, S. Pelzer, W. Wohlleben, FEMS Microbiol. Lett. 163 (1998) 149–157.
[12] H. Seto, T. Kuzuyama, Nat. Prod. Rep. 16 (2000) 589–596.
[13] S.V. Kononova, M.A. Nesmeyanova, Biochemistry (Moscow) 67 (2002) 184–195.
[14] O. Herzberg, C.C. Chen, S. Liu, A. Tempczyk, A. Howard, M. Wei, D. Ye, D. Dunaway Mariano, Biochemistry 41 (2002) 780–787.
[15] G. Zhang, J. Dai, Z. Lu, D. Dunaway-Mariano, J. Biol. Chem. 278 (2003) 41302–41308.
[16] H. Nakashita, K. Kozuka, T. Hidaka, O. Hara, H. Seto, Biochim. Biophys. Acta 1490 (2000) 159–162.
[17] T. Hidaka, M. Goda, T. Kuzuyama, N. Takei, M. Hidaka, H. Seto, Mol. Gen. Genet. 249 (1995) 274–280.
[18] S. Kobayashi, T. Kuzuyama, H. Seto, Antimicrob. Agents Chemother. 44 (2000) 647–650.
[19] P. Coutrot, P. Savignac, Synthesis-Stuttgart (1978) 36–38.
[20] S. Freeman, W.J. Irwin, C.H. Schwalbe, J. Chem. Soc. Perkin Trans. (1991) 263–267.
[21] H. Bisswanger, Enzymkinetik: Theorie und Methoden, 3rd ed., Wiley-VCH, Weinheim, 2000.
[22] S. Bringer-Meyer, K.-L. Schimz, H. Sahm, Arch. Microbiol. 146 (1986) 105–110.
[23] R. Fang, P.F. Nixon, R.G. Duggleby, FEBS Lett. 437 (1998) 273–277.
[24] M. Ibdah, A. Bar-Ilan, O. Livnah, J.V. Schloss, Z. Barak, D.M. Chipman, Biochemistry 35 (1996) 16282–16291.
[25] J. Koga, T. Adachi, H. Hidaka, J. Biol. Chem. 267 (1992) 15823–15828.
[26] G.A. Sprenger, U. Schörken, G. Sprenger, H. Sahm, Eur. J. Biochem. 230 (1995) 525–532.
[27] M. Graupner, H. Xu, R.H. White, J. Bacteriol. 182 (2000) 4862–4867.
[28] A.K. Chang, R.G. Duggleby, Biochem. J. 327 (1997) 161–169.
[29] C.M. Hill, S.S. Pang, R.G. Duggleby, Biochem. J. 327 (1997) 891–898.
[30] A. Kaplun, M. Vyazmensky, Y. Zherdev, I. Belenky, A. Slutzker, S. Mendel, Z. Barak, D.M. Chipman, B. Shaanan, J. Mol. Biol. 357 (2006) 951–963.
[31] S.S. Pang, R.G. Duggleby, R.L. Schowen, L.W. Guddat, J. Biol. Chem. 279 (2004) 2242–2253.
[32] M.S. Hasson, A. Muscate, M.J. McLeish, L.S. Polovnikova, J.A. Gerlt, G.L. Kenyon, G.A. Petsko, D. Ringe, Biochemistry 37 (1998) 9918–9930.
[33] E.S. Polovnikova, M.J. McLeish, E.A. Sergienko, J.T. Burgner, N.L. Anderson, A.K. Bera, F. Jordan, G.L. Kenyon, M.S. Hasson, Biochemistry 42 (2003) 1820–1830.
[34] S. Chakraborty, N.S. Nemeria, A. Balakrishnan, G.S. Brandt, M.M. Kneen, A. Yep, M.J. McLeish, G.L. Kenyon, G.A. Petsko, D. Ringe, F. Jordan, Biochemistry 48 (2009) 981–994.
[35] Y.Y. Chang, A.Y. Wang, J.E. Cronan Jr., J. Biol. Chem. 268 (1993) 3911–3919.
[36] A. Kaplun, E. Binshtein, M. Vyazmensky, A. Steinmetz, Z. Barak, D.M. Chipman, K. Tittmann, B. Shaanan, Nat. Chem. Biol. 4 (2008) 113–118.
[37] J. Koga, Biochim. Biophys. Acta 1249 (1995) 1–13.
[38] A. Schütz, R. Golbik, K. Tittmann, D.I. Svergun, M.H. Koch, G. Hübner, S. König, Eur. J. Biochem. 270 (2003) 2322–2331.
[39] F. Dyda, W. Furey, S. Swaminathan, M. Sax, B. Farrenkopf, F. Jordan, Biochemistry 32 (1993) 6165–6170.
[40] J. Wang, H. Dong, S. Li, H. He, J. Phys. Chem. 109 (2005) 18664–18672.
[41] B. Sedewitz, K.H. Schleifer, F. Götz, J. Bacteriol. 160 (1984) 462–465.
[42] B. Sedewitz, K.H. Schleifer, F. Götz, J. Bacteriol. 160 (1984) 273–278.
[43] P. Neumann, A. Weidner, A. Pech, M.T. Stubbs, K. Tittmann, Proc. Natl. Acad. Sci. U.S.A. 105 (2008) 17390–17395.
[44] P.C. Babbitt, J.A. Gerlt, J. Biol. Chem. 272 (1997) 30591–30594.
[45] P. Arjunan, T. Umland, F. Dyda, S. Swaminathan, W. Furey, M. Sax, B. Farrenkopf, Y. Gao, D. Zhang, F. Jordan, J. Mol. Biol. 256 (1996) 590–600.
[46] D. Dobritzsch, S. König, G. Schneider, G. Lu, J. Biol. Chem. 273 (1998) 20196–20204.
[47] Y. Lindqvist, G. Schneider, U. Ermler, M. Sundstrom, EMBO J. 11 (1992) 2373–2379.
[48] Y.A. Muller, G.E. Schulz, Science 259 (1993) 965–967.
[49] S.S. Pang, R.G. Duggleby, L.W. Guddat, J. Mol. Biol. 317 (2002) 249–262.
[50] R. Breslow, J. Am. Chem. Soc. 80 (1958) 3719–3726.
[51] D. Kern, G. Kern, H. Neef, K. Tittmann, M. Killenberg-Jabs, C. Wikner, G. Schneider, G. Hübner, Science 275 (1997) 67–70.
[52] M. Reynen, H. Sahm, J. Bacteriol. 170 (1988) 3310–3313.
[53] C.F. Hawkins, A. Borges, R.N. Perham, FEBS Lett. 255 (1989) 77–82.
[54] A.K. Chang, P.F. Nixon, R.G. Duggleby, Biochem. J. 339 (1999) 255–260.
[55] J.M. Candy, R.G. Duggleby, Biochim. Biophys. Acta 1385 (1998) 323–338.
[56] G. Schenk, F.J. Leeper, R. England, P.F. Nixon, R.G. Duggleby, Eur. J. Biochem. 248 (1997) 63–71.
[57] C.Y. Huang, A.K. Chang, P.F. Nixon, R.G. Duggleby, Eur. J. Biochem. 268 (2001) 3558–3565.
[58] K. Tittmann, R. Golbik, K. Uhlemann, L. Khailova, G. Schneider, M. Patel, F. Jordan, D.M. Chipman, R.G. Duggleby, G. Hübner, Biochemistry 42 (2003) 7885–7891.
[59] C. Wikner, U. Nilsson, L. Meshalkina, C. Udekwu, Y. Lindqvist, G. Schneider, Biochemistry 36 (1997) 15643–15649.
[60] J.M. Candy, R.G. Duggleby, Biochem. J. 300 (1994) 7–13.
[61] J.P. Fuerste, W. Pansegrau, R. Frank, H. Blocker, P. Scholz, M. Bagdasarian, E. Lanka, Gene 48 (1986) 119–131.
[62] K.E. Nelson, K.E. Weinel, C. Paulsen, I.T. Dodson, R.J. Hilbert, H. Martins dos Santos, V.A. Fouts, D.E. Gill, S.R. Pop, M. Holmes, M. Brinkac, L. Beanan, M. DeBoy, R.T. Daugherty, S. Kolonay, J. Madupu, R. Nelson, W. White, O. Peterson, J. Khouri, H. Hance, I. Chris Lee, P. Holtzapple, E. Scanlan, D. Tran, K. Moazzez, A. Utterback, T. Rizzo, M. Lee, K. Kosack, D. Moestl, D. Wedler, H. Lauber, J. Stjepandic, D. Hoheisel, J. Straetz, M. Heim, S. Kiewitz, C. Eisen, J. Timmis, K.N. Dusterhoft, A. Tummler, B.C.M. Fraser, Environ. Microbiol. 4 (2002) 799–808.
[63] J. Sambrook, E.F. Fritsch, T. Maniatis, Molecular Cloning: A Laboratory Manual, 2nd ed., Cold Spring Harbor Lab. Press, Plainview, NY, 1989.
[64] R.D. Appel, A. Bairoch, D.F. Hochstrasser, Trends Biochem. Sci. 19 (1994) 258–260.
[65] M.M. Bradford, Anal. Biochem. 72 (1976) 248–254.